Sub-laser-cycle electron pulses for probing molecular dynamics

Hiromichi Niikura*, F. Légaré†, R. Hasbani*, A. D. Bandrauk†, Misha Yu. Ivanov*, D. M. Villeneuve* & P. B. Corkum*

** National Research Council of Canada, 100 Sussex Drive, Ottawa, Ontario K1A OR6, Canada*
† Université de Sherbrooke, Sherbrooke PQ, Canada

Experience shows that the ability to make measurements in any new time regime opens new areas of science. Currently, experimental probes for the attosecond time regime (10^{-18}–10^{-15} s) are being established. The leading approach is the generation of attosecond optical pulses by ionizing atoms with intense laser pulses. This nonlinear process leads to the production of high harmonics during collisions between electrons and the ionized atoms. The underlying mechanism implies control of energetic electrons with attosecond precision. We propose that the electrons themselves can be exploited for ultrafast measurements. We use a 'molecular clock', based on a vibrational wave packet in H_2^+ to show that distinct bunches of electrons appear during electron–ion collisions with high current densities, and durations of about 1 femtosecond (10^{-15} s). Furthermore, we use the molecular clock to study the dynamics of non-sequential double ionization.

A substantial effort is under way to develop single attosecond optical pulses[1–3], or trains of attosecond pulses[4–6], using the physical processes occuring in high-harmonic generation[7]. High harmonics are produced during the electron–ion collisions induced by strong-field laser ionization, usually referred to as 'recollision'. Within one optical period an electron is removed from the atom, is driven back when the laser field reverses its direction, and collides with the parent ion. The duration of the electron–ion recollision largely determines the duration of the attosecond photon pulse.

Here we study the recollision electron wave packet, measuring both the probability of recollision and its time structure. Although only one electron is involved in the electron–ion recollision, we adopt the language of electron beams to indicate the potential applications of recollision electrons. These applications are the topic of the final section of this Article.

We characterize the unusually large current density and its time structure as seen by the ion following ionization. To do this, we use H_2 molecules in a low-density gas as a molecular clock. As ionization simultaneously forms two wave packets—one a vibrational wave packet moving on the $H_2^+(X^2\Sigma_g^+)$ surface; the other, the electron wave packet that we wish to study—ionization starts the vibrational clock in H_2^+. We choose H_2^+ as the molecular clock because of the speed of its vibrational wave packet, and because all excited states of H_2^+ directly dissociate. By choosing the molecular axis perpendicular to the laser electric field, we decouple the $X^2\Sigma_g^+$ and $A^2\Sigma_u^+$ surfaces in H_2^+, ensuring that the clock remains accurate in the presence of the field. To read the clock, we observe the kinetic energy of the protons produced by inelastic scattering when the electron recollides with the parent ion. The kinetic energy distribution measures the position of the vibrational wave packet at the time of recollision, and therefore the recollision time. In our experiment the time resolution is ~1 fs.

Next, we apply the molecular clock to follow the subcycle correlated electron dynamics. Non-sequential double ionization (two-electron ionization that cannot be described by two sequential single-electron ionization processes) is a common occurrence during strong-field ionization of atoms or molecules containing two or more electrons[7–13]. We distinguish the double ionization due to recollision from instantaneous double ionization by using the molecular clock, and find that electron recollision dominates others by at least two orders of magnitude. We confirm that the most important route to non-sequential ionization is through the production of excited states by recollision that can later ionize in the strong laser field.

Finally, we compare the double-ionization yield due to recollision in H_2 and helium[8,11,13]. We find that double ionization (excitation) is about ten times more probable in hydrogen molecules than in helium[11,13].

Selecting the fragmentation channel

We now proceed to fully characterize the current density using H_2 double-ionization (excitation) for all aspects of the measurement. (For convenience, we will use 'double-ionization' when referring to either the non-sequential emission of two electrons, or the emission of one and the correlated excitation of the other.)

First, we identify collision-induced excitation or double ionization through the previously observed[14,15] high kinetic energy of the fragment protons that are produced. We show that recollision is responsible for these energetic protons by comparing the kinetic-energy spectrum measured with linear and elliptically polarized light[16]. Second, the ellipticity dependence of the proton yield measures the initial velocity spread of the electron wave packet. With this input, we calculate the current density seen by the newly ionized ion. Third, we confirm the predicted temporal structure by comparing the calculated and measured kinetic-energy spectrum. Finally, we confirm the magnitude of the current density by

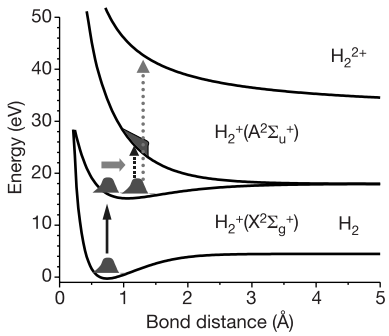

Figure 1 Important potential-energy curves for H_2 and its ions. Ionizing H_2 forms a dual wave packet. One is a vibrational wave packet on the ground (Σ_g) state of H_2^+ (shown). The other is an electron wave packet that moves in the laser field. The vibrational wave packet evolves until H_2^+ is excited by inelastic scattering caused by the returning electron wave packet.

comparing the calculated and measured probability of double ionization.

Figure 1 plots the potential-energy surfaces of molecular hydrogen and its ions. Single ionization (represented as the solid vertical arrow in Fig. 1) results in the formation of two correlated wave packets. One is the electron wave packet that we wish to characterize. The other is a vibrational wave packet moving (horizontal arrow) on the field-modified Σ_g potential-energy surface until electron re-collision occurs.

When the electron wave packet returns to the ion it can inelastically scatter, producing excited states of H_2^+ or further ionizing the ion (dotted arrow in Fig. 1). All excited states of H_2^+ lead to dissociation of the molecular ion. They can be identified through the kinetic-energy spectrum of the protons, provided that the laser field does not further ionize them. To avoid further ionization we keep the light intensity low, and we exploit two additional effects: that ionization is not enhanced for perpendicular orientation[17], and that ionization is suppressed for anti-symmetric states[18]. The kinetic energy spectrum gives us a relatively uncomplicated 'time history' of the recollision dynamics. The channel of interest produces fragments with kinetic energy in the range 1–10 eV.

We performed the experiment in a time-of-flight mass spectrometer containing H_2 molecules at a pressure of 10^{-6} torr. We apply a uniform electric field across two parallel electrodes separated by 3 cm. A 1-mm-diameter hole in one electrode allows us to observe protons only from those molecules whose axis lies close to parallel with respect to the time-of-flight axis. The signal is measured on a microchannel plate detector.

Although we could observe molecules with any orientation, we concentrate on those that are oriented perpendicular to the laser polarization. H_2^+ cannot change its orientation[19] in the brief interval between ionization, recollision and dissociation. The collection half-angle depends on the dissociation velocity of the fragments and the applied electric field. For our experimental conditions, the half angle was 8° at 10 eV with the angle increasing with the inverse of the velocity.

H_2 molecules are ionized by a 50-fs light pulse of 800 nm wavelength, propagating perpendicular to the time-of-flight axis and focused to a peak laser intensity of $(1.5 \pm 0.5) \times 10^{14}\,\mathrm{W\,cm^{-2}}$. The intensity is calibrated against the ionization of xenon[20]. At this intensity the recollision electron should have maximum collision energy of ~30 eV, sufficient only to excite $X^2\Sigma_g^+ \rightarrow A^2\Sigma_u^+$ in the molecular ion. To change the ellipticity of the laser light we rotate a half-wave plate that is placed before a fixed quarter-wave plate. This procedure preserves the direction of the major axis as the ellipticity changes. We now proceed to identify the signature of recollision in the kinetic-energy spectrum.

Confirming recollision

Figure 2 plots the measured kinetic energy spectrum of the protons. The main plot, shown on a very-much-expanded vertical scale, is for molecules oriented perpendicular to the field direction, whereas the inset is for molecules oriented in the parallel direction. Because of its scale, the main plot of Fig. 2 most clearly shows the low-probability events, namely the protons with high kinetic energy.

To identify the channel of interest, we must distinguish it from other dissociation channels that influence the kinetic-energy spectrum of the protons. Bond softening[21,22], which originates from the mixing of the Σ_g and Σ_u levels by the laser field, is responsible for the kinetic-energy peak near 0.5 eV, clearly seen in Fig. 2 inset. To eliminate bond-softened molecules, we select perpendicularly oriented molecules where Σ_g and Σ_u are decoupled. Enhanced ionization, which refers to the large and broad increase in ionization rate with the internuclear coordinate in the region where the bond breaks[17,23,24], is responsible for the peak in the ~2.5 eV region. Like bond softening, it is also eliminated for perpendicular molecules[18].

We confirm, by measuring the number of protons as a function of the ellipticity of the laser light[1,10,12,16], that recollision is responsible for the high-kinetic-energy protons. Processes caused by electron recollision are very sensitive to small deviations from linear polarization[7]. The inset in Fig. 3 illustrates the method that we use. In linearly polarized light, the laser field dominates the electron motion in the direction of the laser polarization. However, the quantum-mechanical uncertainty of the electron's velocity at the time of ionization causes the electron wave packet to have expanded significantly in the lateral direction by the time it re-collides with the ion (Fig. 3 inset). We can easily influence the electron trajectory by adding a small ellipticity to the laser pulse. The weak perpendicular field pushes the electron wave packet to the side so that recollision becomes impossible.

The sensitivity to ellipticity is seen in Fig. 2. The upper curve is obtained using linearly polarized light, and the lower curve is obtained using light with ellipticity of $E_y/E_x = 0.3$ (where E_y (E_x) is the laser electric field in the direction perpendicular (parallel) to the molecular axis). Ellipticities between 0 and 0.3 occupy the intermediate region, whereas the lower curve is essentially unchanged for higher ellipticities. The difference of data counts between the upper and lower curves determines the kinetic-energy

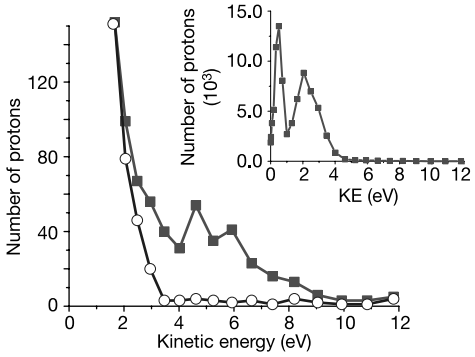

Figure 2 The number of protons measured per unit energy as a function of the proton kinetic energy. The upper curve is obtained with linear polarized light, whereas the lower curve is obtained with elliptically polarized light (ellipticity $E_y/E_x = 0.3$; E_x and E_y are defined in the text). Intermediate ellipticities fall between these curves. The main plot is for perpendicularly aligned molecules, the inset is for molecules aligned parallel to the laser field (KE, kinetic energy).

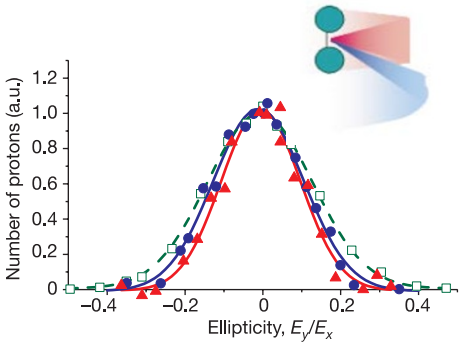

Figure 3 Ellipticity dependence of the number of energetic protons produced when an intense laser field ionizes H_2. Such narrow ellipticity dependence is characteristic of inelastic scattering between the recollision electron and the ion. The data is for H_2 aligned both parallel (blue filled circles) and perpendicular (red filled triangles) to the laser field. For comparison purposes, the ellipticity dependence of the double-ionization probability of argon, an atom with almost the same ionization potential, is shown (open green squares). The inset illustrates that elliptically polarized light can redirect the electron so that recollision becomes impossible (see text). (a.u., arbitrary units.)

spectrum of protons produced by recollision, as we will show below. It is clear from Fig. 2 that our measurements should concentrate on kinetic energies above about 4 eV.

Figure 3 shows the ellipticity dependence of the recollision yield. All high-kinetic-energy fragments have the same ellipticity dependence. At each ellipticity, we integrate the signal count in the kinetic energy range 4–9 eV. The three curves included in Fig. 3 are for argon and for H_2 molecules aligned parallel and perpendicular to the laser polarization.

Lateral spread of the electron wave packet

The velocity that the electron acquires in the direction perpendicular to the laser field during ionization determines the expansion of the electron wave packet in the lateral direction. If the velocity is large, the wave packet that recollides is spread over a large area. We concentrate on the lateral velocity for molecules aligned perpendicular to the laser field.

As the laser ellipticity increases, the electron wave packet is pushed further from the ion core in the direction of the minor component of the laser field. When the electron wave packet returns to the ion core for the first time, at a time $\Delta t = 1.8$ fs after its birth, its displacement is given by $dx \approx 5.14\varepsilon E/m\omega^2$ (ref. 12), where ε is ellipticity, E is the strength of laser field, m is the electron mass and ω is the laser angular frequency. Our 1/e width $\varepsilon = 0.14$ yields a $1/e$ displacement $dx = 7.7$ Å. Because the effective collision cross-section is small (~ 1 Å^2), the displacement allows us to measure the spatial distribution of the electron wave packet when it returns to the ion core[12]. From this distribution, we determine that the initial velocity spread at the time of ionization is ~ 4.2 Å fs^{-1}. The observed ellipticity dependence shows a gaussian form, as predicted by tunnelling theory[25]. Argon is used as a reference that we can accurately calculate. For argon (open squares in Fig. 3) the same procedure yields ~ 5.6 Å fs^{-1}, in excellent agreement with 5.4 Å fs^{-1} predicted by the atomic tunnelling theory[25].

Knowledge of both the expansion velocity of the electron wave packet and its shape provides the initial conditions for a semi-classical simulation of the electron dynamics following ionization[13]. In the calculation, we follow many electron trajectories in two dimensions; each trajectory is characterized by different initial positions and velocities and by a weight ρ_I, which reflects the probability of that trajectory. We count the number of trajectories passing through the surface of a circle of radius r_0, where πr_0^2 is the inelastic cross-section (ref. 26 and ⟨http://physics.nist.gov/PhysRefData/Ionization/Xsection.html⟩) for the $\Sigma_g \rightarrow \Sigma_u$ transition in H_2^+, within a unit time. In the calculations, we correct the atomic tunnelling[27] rate to include the molecular structure. We also include the influence of the molecular ion's field on the free electron trajectories.

Figure 4 is a plot of the calculated current density experienced by the molecular ion. Only electrons with energy greater than the resonant energy between Σ_g and Σ_u are included in this plot. Otherwise, the current density includes all other electrons that pass through the collisional surface of area πr_0^2. Figure 4 shows that the recollision current consists of five micro-bunches. The current density rises in the second half-period after ionization, reaching 8×10^{10} A cm^{-2}. At later times, the amplitude decreases rapidly. Such high current densities are available only from very large accelerators such as SLAC.

Temporal structure of the electron wave packet

To confirm the time structure of the recollision, we turn our attention to the vibrational wave packet. The laser parameters place our experiment in the regime where ionization can be calculated by assuming that the electron tunnels through the barrier caused by the superposition of the laser field and the ion field[27,28]. Removing an electron from H_2 forms a vibrational wave packet on the ground Σ_g of H_2^+ that resembles the ground-state wavefunction. Ionization simultaneously releases the electron wave packet that we have been discussing. The distortion of the vibrational wave packet compared to the ground-state wavefunction of H_2 (ref. 29) owing to the dependence of the ionization rate on the internuclear separation is included in the calculation.

We follow the H_2^+ wave packet by solving Schrödinger's equation on the Σ_g molecular potential. By including the interaction of the laser field with the perpendicular induced dipole, we confirm that, at this intensity, other states have a negligible effect on the motion of the wave packet. The proton kinetic-energy spectrum resulting from recollision is obtained by projecting the Σ_g wave packet onto the Σ_u continuum wavefunctions.

Figure 5 (solid line) shows the incoherent sum of the kinetic-energy spectra of protons produced by all five micro-bunches weighted according to their relative probabilities as determined by the calculated time-independent current density in Fig. 4, and weighted by the cross-section at the average internuclear separation[26] for each micro-bunch. We have used angle-averaged cross-sections because, to our knowledge, no cross-section data are available for oriented molecules. We show the individual contribution of the first and third recollision as dotted lines. Their time separation is 2.7 fs. It is clear from Fig. 5 that we can resolve contributions from an intermediate electron pulse.

The experimental kinetic energy spectrum (data points) is also plotted in Fig. 5. In the vertical direction, error bars are determined by shot-to-shot statistics. The error in the horizontal direction is only dependent on the measurement resolution (500 ps) of the time-of-flight mass spectrometer. The error is of the order of the spacing of the data points. To obtain the experimental data for Fig. 5, the kinetic-energy spectrum, measured with elliptically polarized light (Fig. 2, circles), was subtracted from the kinetic-energy spectrum measured with linearly polarized light (Fig. 2, squares).

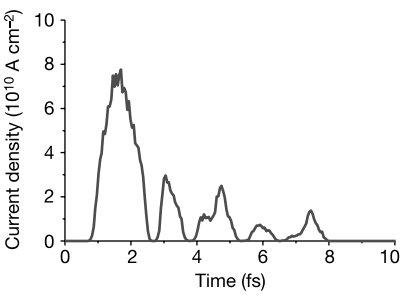

Figure 4 The calculated electron current density experienced by the ion as a function of time after ionization. Only electrons with sufficient energy for inelastic scattering are included.

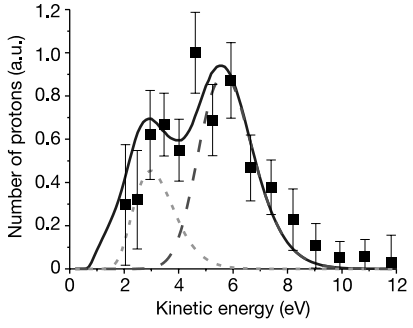

Figure 5 Observed (data points) and calculated (solid curve) kinetic-energy spectrum for the energetic protons caused by inelastic scattering. The agreement confirms the time dependence of the current density. The dashed lines show the contributions from the first (long dash) and third electron micro-bunch (short dash).

This procedure distinguishes the processes due to recollision from other sources.

The overlap between the calculation and the experiment in Fig. 5 is notable. We stress that our ability to measure the ~1-fs duration of the first micro-bunch is achieved because of the double correlation between the electronic and vibrational wave packets. We do not use either time-dependent polarization[1] or a few-cycle pulse[2,3].

Magnitude of the electron current density

In Fig. 5, we account for the relative magnitude of each recollision peak. The only free parameter is the overall normalization of the experimental kinetic-energy spectrum with respect to the theoretical one. Theoretically, using the current density in Fig. 4 and the angle-averaged cross-section, we can predict the angle-averaged probability that one single-ionization event will lead to inelastic excitation of Σ_u. At $1.5 \times 10^{14}\,W\,cm^{-2}$, we calculate that 7% of all ionization events result in inelastic scattering. This establishes the vertical scale in Fig. 5 for the calculations. We now establish this experimentally.

The number of protons produced by recollision is plotted in Fig. 6 as a function of the alignment of the molecular axis with respect to the laser field. There are about 10 times more inelastic scattering events for molecules aligned parallel to the field than perpendicular. Were we able to align all molecules relative to the laser polarization, we could separate the influence of angle-dependent ionization rates and cross-sections. But owing to the small asymmetry in the polarizability and the large rotational constant, alignment is not possible.

Figure 7 shows the branching ratio between H_2^+ (circles), bond softening (0–0.9 eV, upward pointing triangles), enhanced ionization (0.9–4 eV, downward pointing triangles) and inelastic scattering (>4 eV, squares). To obtain this branching ratio, we measure the probability of each product channel at 10° intervals. This establishes the probability as a function of angle. Then we integrate each channel over all 4π steradians. The branching ratio of each channel is obtained by dividing each probability by the sum of all channels. The experimental branching ratio into inelastically scattered fragments is ~2–3% at $1.5 \times 10^{14}\,W\,cm^{-2}$. This establishes the vertical scale in Fig. 5 for the measurement. As with helium, double ionization is almost independent of the laser intensity[11,13].

Both the calculation and the measurement have a degree of uncertainty. By assigning a fragment kinetic energy >4 eV to inelastic scattering, we experimentally underestimate the true branching ratio into inelastic channels. We know that, at least for perpendicular molecules (Fig. 2), about 30% of all inelastic events lead to protons with kinetic energy in the 2–4 eV range. But if the molecule is oriented parallel to the internuclear axis, such events are overwhelmed by the enhanced ionization peak and we cannot accurately measure them. Theoretically, we overestimate the experimental branching ratio by using hard-sphere[13], angle-averaged cross-sections and two-dimensional trajectories. In view of these uncertainties, the experiment and calculation agree.

Strong-field non-sequential double ionization

Of the phenomena observed in the interaction between atoms/molecules and ultrashort intense laser pulses (high-harmonic generation[30,31], very-high-energy electron production[32,33], and non-sequential double ionization[8,10,11]), all but the last can be described with a single active electron[11]. Thus non-sequential double ionization gains a particular significance within strong-field physics, connecting it to multi-electron physics, a subject that is important in many other areas of science. There are a number of important issues in non-sequential double-ionization physics that our experiment allows us to comment on.

Multi-electron dynamics. Although we have expressed our results in terms of the current density and concentrated on the electron that recollides, we obtain the current by measuring the correlated-electron dynamics during strong-field ionization. Until recently, the basic mechanism responsible for double ionization was a subject of controversy[11]. Strong-field double ionization was initially thought to be caused by shake-off[8]—the departing electron causes the remaining electron to become unbound. It is now accepted that recollision is the main mechanism responsible for double ionization. However, previous experimental measurements were not precise enough to eliminate the possibility that shake-off (or other instantaneous double-ionization processes that are important for X-ray double ionization) plays a minor role.

The double correlation of vibrational and electron wave packet in H_2 allows instantaneous double ionization to be identified, as it would place the H_2^+ on an excited surface before any nuclear motion could occur in the Σ_g. Referring to Fig. 2, we do not observe protons with kinetic energy above ~9.5 eV. The lack of energetic protons with kinetic energy greater than 10 eV implies that, at an intensity of $1.5 \times 10^{14}\,W\,cm^{-2}$, the branching ratio into instantaneous double ionization cannot exceed 10^{-4}.

However, we do resolve in time the decay of the electron–electron interaction in H_2 during ionization in a strong field. Following ionization, the interaction has the complex temporal structure similar to the electron current density in Fig. 4.

The role of excited states. The unique advantage of H_2 is that all excited states of H_2^+ are unstable. Therefore the kinetic-energy spectrum of the fragments can identify the dissociation channels. We find that excited states dominate H_2 double ionization in the intensity regime in which we work. At higher intensities, the Σ_u state would ionize during the laser pulse, making it an important pathway to double ionization. The role of excitation as a route to double

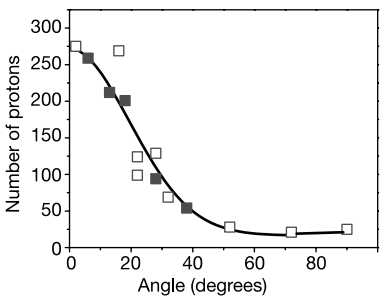

Figure 6 Angular dependence of the double-ionization (excitation) probability due to recollision. Data were taken from 40° on one side of parallel to 90° on the other side to ensure that the results were symmetric. All data points are included in the figure. Filled data points represent data on one side (0 to −40°) and the open points represent the other side (0 to 90°). Inelastic scattering is about 10 times more likely for a molecule aligned parallel to the field than for a molecule aligned perpendicular to the field.

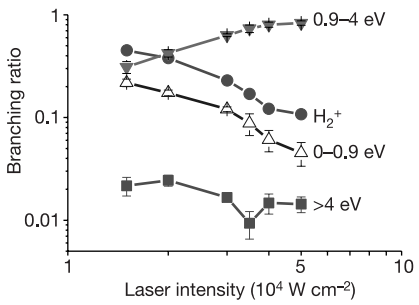

Figure 7 Intensity dependence of the double-ionization (excitation) probability. As with helium, the double-ionization probability (squares) is almost independent of the laser intensity in the non-sequential range. The other channels are bond softening (upward-pointing triangles), enhanced ionization (downward pointing triangles) and H_2^+ (circles).

ionization in atoms has been the subject of considerable speculation[13,34,35].

The significance of alignment in molecular ionization. The transverse velocity spread of the electron as it leaves the atom (molecule) determines the probability of all recollision processes (high-harmonic generation, double ionization and elastic scattering). The data in Fig. 3 allow us to make three important observations about the transverse velocity spread. First, for either alignment of the molecule with respect to the laser polarization, the ellipticity dependence shown in Fig. 2 is independent of the kinetic energy of the fragments in the range caused by recollision (4–9 eV), and is therefore independent of which micro-pulse leads to the excitation. Second, the ellipticity dependence is slightly different for the parallel and perpendicular orientation of the molecules. The transverse velocity spread perpendicular to the laser field therefore depends slightly on the molecular alignment with respect to the laser field. For molecules aligned parallel to the laser polarization, the l/e width of the velocity distribution is 5.0 Å fs^{-1}, while, for perpendicular aligned molecules, the l/e width of the velocity distribution is 4.2 Å fs^{-1}. Third, although Ar has almost the same ionization potential as H_2, the l/e width of the transverse velocity of Ar ($\sim$5.6 Å fs^{-1}) is larger than that for either orientation of H_2.

In contrast to atomic tunnelling theory[25], there have been no theoretical predictions of the electron wave packet spread in molecules. Qualitatively, in agreement with our measurements, we might expect a smaller spread from the broader tunnel that characterizes a perpendicular molecule.

The probability of double ionization (excitation). Although both H_2 and helium have two electrons, the probability of double ionization or excitation is about 10 times higher for H_2 than for He (ref. 11). It is also significantly greater for H_2 than for neon[36], although neon has many more electrons.

Using attosecond electrons for probing

Implicit in our results is the potential to exploit recollision electrons in a number of subfields of gas-phase molecular science operating on all timescales. Currently it is assumed that attosecond science will be an extension of ultrashort-pulse science in a new time regime. However, extreme ultraviolet attosecond pulses are not generated in a laser system but in a very inefficient process involving 'free' electrons[2,3]. Focusing the attosecond extreme ultraviolet radiation onto another gas is also inefficient. In contrast, attosecond electron bunches are produced with $\sim$100% efficiency, and have a high probability of interaction. It seems likely that attosecond science will use attosecond electron pulses and attosecond photon pulses equally. In addition, the technology needed for producing and using attosecond electron bunches is available in many laboratories. We have used a 50-fs laser to produce an electron micro-bunch that has a duration of $\sim$1 fs. This is possible because we exploit correlation—we probe only those molecules that undergo ionization.

If it is necessary to eliminate the weaker micro-bunches and reach individual bunches of electrons, we can borrow two approaches that have been proposed to reach single attosecond optical pulses. One approach uses a few-cycle visible pulse to confine the time of ionization, and to ensure that the driving pulse is terminated before a second recollision is likely[2,3]. The other approach exploits a fundamental pulse with time-dependent polarization to control the electron trajectory[1]. With time-dependent polarization, recollision is only possible for a fraction of the driving laser period, resulting in attosecond extreme ultraviolet pulses and attosecond recollisions.

But what are the implications for conventional femtosecond science? Conventional femtosecond science has no convenient short-wavelength source, although there is a great deal of interest in creating one using X-rays[37] or electrons[38]. Recollision electrons can play that role. Depending on the wavelength of the laser light that creates them, recollision electrons can have very high energies. These electrons are produced when and where they are needed. In effect, they are 'slaved' with attosecond precision to the optical beam that created them. Controlling the laser pulse controls the electrons, both their production and their subsequent motion[39,40].

As probes in femtosecond experiments, recollision electrons are expected to have unique advantages over laser photons. The most important advantage arises during elastic scattering. If the electrons are sufficiently energetic, an image of the structure of the molecule is impressed onto the diffracted electron distribution. Although the recollision electron probes the ion a few femtoseconds after ionization (for most molecules), there is no time for the structure of the neutral molecule to change. Therefore, although the ion is probed, the structure of the neutral molecule is imaged.

Even when time resolution is not an issue, recollision electrons will find applications. For example, in a gas that combines a mixture of excited and unexcited molecules, the intense laser field that is used to create the recollision electrons will preferentially ionize the excited molecules—exactly the molecules that we wish to observe. As the recollision electron probes only its parent, excited molecules will be preferentially imaged.

Few molecules will be needed for imaging, because the current densities are so large. In fact, there is a substantial effort under way to develop methods for single-molecule imaging or few-molecule imaging[40]. The very large current densities that characterize recollision events suggest that recollision electrons could contribute to this effort. □

Received 20 December 2001; accepted 30 April 2002; doi:10.1038/nature00787.

1. Corkum, P. B., Ivanov, M. Yu. & Burnett, N. H. Sub-femtosecond pulses. *Opt. Lett.* **19,** 1870–1872 (1994).
2. Drescher, M. *et al.* X-ray pulses approaching the attosecond frontier. *Science* **291,** 1923–1927 (2001).
3. Hentschel, M. *et al.* Attosecond metrology. *Nature* **414,** 509–513 (2001).
4. Antoine, P., L'Huillier, A. & Lewenstein, M. Attosecond pulse trains using high-order harmonics. *Phys. Rev. Lett.* **77,** 1234–1237 (1996).
5. Paul, P. M. *et al.* Observation of a train of attosecond pulses from high harmonic generation. *Science* **292,** 1689–1692 (2001).
6. Papadogiannis, N. A., Witzel, B., Kalpouzous, C. & Charalambidis, D. Observation of attosecond light localization in higher order harmonic generation. *Phys. Rev. Lett.* **83,** 4289–4292 (1999).
7. Corkum, P. B. A plasma perspective on strong field multiphoton ionization. *Phys. Rev. Lett.* **71,** 1994–1997 (1993).
8. Fittinghoff, D. N., Bolton, P. R., Chang, B. & Kulander, K. C. Observation of nonsequential double ionization of helium with optical tunneling. *Phys. Rev. Lett.* **69,** 2642–2645 (1992).
9. Weber, Th. *et al.* Correlated electron emission in multiphoton double ionization. *Nature* **405,** 658–661 (2000).
10. Bhardwaj, V. R., Rayner, D. M., Villeneuve, D. M. & Corkum, P. B. Quantum interference effects in double ionization and fragmentation of C_6H_6. *Phys. Rev. Lett.* **87,** 253003-1–253003-4 (2001).
11. Walker, B. *et al.* Precision measurement of strong field double ionization of helium. *Phys. Rev. Lett.* **73,** 1227–1230 (1994).
12. Dietrich, P., Burnett, N. H., Ivanov, M. Yu. & Corkum, P. B. High harmonic generation and correlated two electron multiphoton ionization with elliptically polarized light. *Phys. Rev. A* **50,** 3585–3588 (1994).
13. Yudin, G. L. & Ivanov, M. Yu. Physics of correlated double ionization of atoms in intense laser fields: Quasistatic tunneling limit. *Phys. Rev. A* **63**, 033404-1–033404-14 (2001); erratum *Phys. Rev. A* **64**, 019902 (2001).
14. Trump, C., Rottke, H. & Sandner, W. Strong-field photoionization of vibrational ground-state H_2^+ and D_2^+ molecules. *Phys. Rev. A* **60,** 3924–2928 (1999).
15. Staudte, A. *et al.* Observation of a nearly isotropic, high energy Coulomb explosion group in the fragmentation of D_2 by short laser pulses. *Phys. Rev. A* **65,** 020703-1–02070-4 (2002).
16. Sakai, H. *et al.* Non-sequential double ionization of D_2 molecules with intense 20 fs pulses. *Phys. Rev. Lett.* (submitted).
17. Constant, E., Stapelfeldt, H. & Corkum, P. B. Observation of enhanced ionization of molecular ions in intense laser fields. *Phys. Rev. Lett.* **76,** 4140–4143 (1996).
18. Muth-Böhm, J., Becker, A. & Faisal, F. H. M. Suppressed molecular ionization for a class of diatomics in intense femtosecond laser fields. *Phys. Rev. Lett.* **85,** 2280–2283 (2000).
19. Ellert, Ch. & Corkum, P. B. Disentangling molecular alignment and enhanced ionization in intense laser fields. *Phys. Rev. A* **59,** R3170–R3173 (1999).
20. Hankin, S., Villeneuve, D. M., Corkum, P. B. & Rayner, D. M. Nonlinear ionization of organic molecules in high intensity laser fields. *Phys. Rev. Lett.* **84,** 5082–5085 (2000).
21. Zavriyev, A., Bucksbaum, P. H., Muller, H. G. & Schumacher, D. W. Ionization and dissociation in H_2 in intense laser fields at 1.064 μm, 532 nm and 355 nm. *Phys. Rev. A* **42,** R5500–R5513 (1990).
22. Zavriyev, A., Bucksbaum, P. H., Squier, J. & Salin, F. Light-induced vibrational states in H_2^+ and D_2^+ in intense laser fields. *Phys. Rev. Lett.* **70,** 1077–1080 (1993).
23. Seideman, T., Ivanov, M. Yu. & Corkum, P. B. The role of electron localization in intense field molecular ionization. *Phys. Rev. Lett.* **75,** 2819–2822 (1995).
24. Zuo, T. & Bandrauk, A. D. Charge-resonance-enhanced ionization of diatomic molecular ions by intense lasers. *Phys Rev. A* **52,** R2511–R2514 (1995).

25. Delone, N. B. & Krainov, V. P. Energy and angular electron spectra for the tunnel ionization of atoms by strong low-frequency radiation. *J. Opt. Soc. Am. B* **8,** 1207–1212 (1991).
26. Peek, J. M. Inelastic scattering of electrons by the hydrogen molecular ion. *Phys. Rev.* **134,** A877–A883 (1964).
27. Ammosov, M. V., Delone, N. B. & Krainov, V. P. Tunnel ionization of complex atoms and of atomic ions in an alternating electromagnetic field. *Zh. Eksp. Teor. Fiz.* **91**, 2008–2013 (1986); *Sov. Phys. JETP* **64**, 1191–1194 (1989).
28. Keldysh, L. V. Ionization in the field of a strong electromagnetic wave. *J. Exp. Theor. Phys.* **47,** 1945–1957 (1964).
29. Dietrich, P., Ivanov, M. Yu., Ilkov, F. & Corkum, P. B. Two-electron dissociative ionization of H_2 and D_2 in infrared fields. *Phys. Rev. Lett.* **77,** 4150–4153 (1996).
30. Macklin, J. J., Kmetic, J. D. & Gordon, C. L. High-order harmonic generation using intense femtosecond pulses. *Phys. Rev. Lett.* **70,** 766–769 (1993).
31. Bartels, R. *et al.* Shaped-pulse optimization of coherent emission of high-harmonic soft X-rays. *Nature* **406,** 164–166 (2000).
32. Mohideen, U. *et al.* High intensity above-threshold ionization of He. *Phys. Rev. Lett.* **71,** 509–512 (1993).
33. Paulus, G. G., Nicklich, W., Xu, H., Lambropoulos, P. & Walther, H. Plateau in above threshold ionization spectra. *Phys. Rev. Lett.* **72,** 2851–2854 (1994).
34. Feuerstein, B. *et al.* Separation of recollision mechanisms in nonsequential strong field double ionization of Ar: The role of excitation tunneling. *Phys. Rev. Lett.* **87,** 043003–043007 (2001).
35. Becker, A. *et al.* Laser-induced inner shell vacancies in double ionized argon. *J. Phys. B* **33,** L547–L552 (2000).
36. Bhardwaj, V. R. *et al.* Few cycle dynamics of multiphoton double-ionization. *Phys. Rev. Lett.* **86,** 3522–3525 (2001).
37. Rischel, C. *et al.* Femtosecond time-resolved X-ray diffraction from laser-heated organic films. *Nature* **390,** 490–492 (1997).
38. Ihee, H. *et al.* Direct imaging of transient molecular structures with ultrafast diffraction. *Science* **291,** 458–462 (2001).
39. Ivanov, M. Yu., Corkum, P. B., Zuo, T. & Bandrauk, A. D. Routes to control of intense-field atomic polarizability. *Phys. Rev. Lett.* **74,** 2933–2937 (1995).
40. Neutze, R. *et al.* Potential for biomolecular imaging with femtosecond X-ray pulses. *Nature* **406,** 752–757 (2000).

Acknowledgements

F.L. acknowledges financial support from Canada's Natural Science and Engineering Research Council, the Canadian Institute for Photonics Innovation and Quebec's Fonds pour la Formation des Chercheurs et l'Aide à la Recherche.

Competing interests statement

The authors declare that they have no competing financial interests.

Correspondence and requests for materials should be addressed to P.B.C. (e-mail: Paul.Corkum@nrc.ca).